Received: 25 October 2024 | Revised: 20 February 2025 | Accepted: 11 March 2025

https://doi.org/10.1016/j.jtha.2025.03.012

ORIGINAL ARTICLE

Discerning specific thrombolytic activities and blood clot degradomes of diverse snake venoms with untargeted peptidomics

Cara F. Smith[1,2] | Mamadou Alpha Baldé[2,3] | Stephanie French[4] | Cassandra M. Modahl[4] | Lilyrose Bahrabadi[1] | Merilyn Amponsah-Asamoah[1] | Keira Y. Larson[1] | Sean P. Maroney[1] | David Ceja Galindo[1] | Martin Millimouno[2,3] | Naby Camara[2,3] | Jordan Benjamin[2] | Nicklaus P. Brandehoff[2,5] | Maxwell C. McCabe[1] | Mitchell J. Cohen[6] | Kate Jackson[2,7] | Cellou Baldé[2,3] | Todd A. Castoe[8] | Stephen P. Mackessy[9] | Kirk C. Hansen[1] | Anthony J. Saviola[1]

[1]Department of Biochemistry and Molecular Genetics, University of Colorado Denver, Aurora, Colorado, USA

[2]Asclepius Snakebite Foundation, Aurora, Colorado, USA

[3]Snakebite Center of Excellence, Institut de Recherche en Biologie Appliqueé de Guinée (IRBAG), Kindia, Guinea

[4]Department of Tropical Disease Biology, Centre for Snakebite Research and Interventions, Liverpool School of Tropical Medicine, Liverpool, United Kingdom

[5]Rocky Mountain Poison and Drug Center, Denver Health and Hospital Authority, Denver, Colorado, USA

[6]Department of Surgery, University of Colorado Denver, Aurora, Colorado, USA

[7]Biology Department, Whitman College, Walla Walla, Washington, USA

[8]Department of Biology, University of Texas at Arlington, Arlington, Texas, USA

[9]Department of Biological Sciences, University of Northern Colorado, Greeley, Colorado, USA

Correspondence
Anthony J. Saviola, Department of Biochemistry and Molecular Genetics,

Abstract

Background: Many snake venoms have been shown to possess thrombolytic activity. However, it remains unclear if actions on other clot-stabilizing proteins beyond fibrin chains contribute significantly to venom-induced thrombolysis because the clot-wide targets of venom proteases and the mechanisms responsible for thrombolysis are not well understood.

Objectives: Here, we utilized a high-throughput, time-based thrombolysis assay in combination with untargeted peptidomics to provide comprehensive insight into the effects of venom from 5 snake species on blood clot degradation.

Methods: We compared thrombolytic profiles across venoms with variable levels of proteases and generated venom-specific fingerprints of cleavage specificity. We also compared the specific effects of venoms that possess a range of thrombolytic activity on fibrin chains and other clot-bound proteins involved in clot structure.

Results: Protease-rich venom more effectively degraded blood clots. Venoms with higher thrombolytic activity demonstrated an enhanced ability to target multiple sites across fibrin chains critical to clot stability and structure, as well as clot-stabilizing proteins including factor XIII, fibronectin, and vitronectin.

Conclusion: Collectively, this study significantly expands our understanding of the thrombolytic and fibrinolytic effects of snake venom by determining the full suite of clot-specific venom targets that are involved in clot formation and stability. This has

Manuscript handled by: Ton Lisman

Final decision: Ton Lisman, 11 March 2025

12801 East 17th Avenue, University of Colorado Denver, Aurora, CO 80045, USA.
Email: Anthony.Saviola@cuanschutz.edu

Funding information
This work was supported by Department of Defense (DoD) grant ID07200010-301-35 to A.J.S., C.F.S., and N.P.B. and the Fulbright U.S. Scholar Grant to C.F.S.

important implications for the treatment of snake envenomation, the bioprospecting of therapeutically useful molecules, and the development of research tools for investigating hematologic disorders.

KEYWORDS
fibrin, fibrinolysis, proteomics, snake venoms, thrombosis

1 | INTRODUCTION

Snake venom toxins that interfere with hemostatic processes have remained an enduring focus in snake venom research [1–4], and a myriad of procoagulant, anticoagulant, and fibrinolytic effects of various venoms and their toxins have been demonstrated experimentally and clinically across venomous snakes [5–7]. Identification and characterization of these toxins and their activities have important implications for treating snake envenomation, the bioprospecting of therapeutically useful molecules, and the development of research tools for investigating hematologic disorders [8]. Although snake venoms are mixtures of both enzymatic and nonenzymatic toxins that can act synergistically to produce a range of biological effects [9,10], much of the hematological disruption that results from snakebite is due to the action of enzymes belonging to the snake venom metalloprotease (SVMP) and snake venom serine protease (SVSP) families [11–13]. These protease families are typically abundant in viper venoms and have a variety of target substrates in plasma, the extracellular matrix, and the basement membrane components of capillaries [11,12,14–18]. Because of these activities, proteolytically rich venoms tend to promote defibrination, extravasation, capillary rupture, and hemotoxicity, resulting in local and/or systemic hemorrhage [12,19], and represent key contributors to human morbidity and mortality associated with snakebite worldwide [5,20].

In addition, to pro- and anticoagulant properties, snake venoms and isolated venom proteins have demonstrated thrombolytic activity *in vitro* and *in vivo* [21–23], and many proteins involved specifically in thrombus formation and stability, including fibrin(ogen), fibronectin (FN1), and other structural proteins, coagulation factors, complement components, and plasminogen, have been identified as substrates of venom toxins [14–17,24]. However, it remains unclear if the activity of snake venoms on other clot-stabilizing proteins beyond fibrin chains contributes significantly to the thrombolytic activity of snake venoms because the clot-wide targets of venom proteases and the mechanisms responsible for thrombolysis have yet to be fully investigated.

A detailed understanding of full protease substrate profiles (degradomes) is critical for understanding their overall function and possible contributions to disease pathophysiology [25]. Recently, peptidomic approaches have gained traction in the study of disease progression and the discovery of disease state biomarkers [26]. Peptidomics involves studying all peptides resulting from proteolysis and characterizing specific cleavage sites to understand enzyme-substrate target specificity. Peptidomics has been utilized to discover novel substrates of previously characterized proteases [27] and to detect disease biomarkers and predictors of clinical outcomes [28,29]. Accordingly, peptidomics can be utilized as a valuable complement to proteomics to facilitate the linkage of peptide-level changes with physiological responses, disease state, and pathophysiology [30].

The broad motivation of this study was to gain new insights into the dynamics of venom-induced thrombolysis through detailed characterization of the clot degradome produced by snake venom and how this might vary across different species. We utilized a high-throughput, time-based thrombolysis assay combined with untargeted peptidomics to comprehensively assess the effects of venom from 5 snake species on blood clot degradation. First, we compared thrombolytic profiles across venoms with variable levels of proteases and generated venom-specific fingerprints of cleavage specificity. We then identified and compared the specific effects of highly thrombolytic and less thrombolytic venoms on fibrin chains and other clot-bound proteins involved in clot structure. Our findings provide critical new insight for understanding the mechanisms responsible for thrombolysis and other hemostatic events triggered by snake venom proteases and demonstrate the power of protease substrate profiling for identifying the distinct activities and pathophysiological effects of venom toxins.

2 | METHODS

2.1 | Halo thrombolytic assay

Blood samples were collected and pooled from healthy adult volunteers who gave informed consent to participate in the study per the Declaration of Helsinki. Blood was collected into trisodium citrate (3.2%) tubes via venipuncture, and clot formation was induced with the recombinant tissue factor Dade Innovin. Innovin was reconstituted into 10 mL of double-distilled water according to the manufacturer's instructions. A clotting mixture of 15% (v/v) Innovin and calcium chloride (67 mM) in 2-[4-(2-hydroxyethyl)piperazin-1-yl]ethanesulfonic acid buffer (25 mM 2-[4-(2-hydroxyethyl)piperazin-1-yl]ethanesulfonic acid, 137 mM sodium chloride) was prepared as previously described [31]. Five microliters of clotting mixture was pipetted onto the bottom edge of a flat-bottomed, tissue culture–treated 96-well plate. This clotting mixture was spread in a circular motion around the edge of the well before adding 25 μL of blood to form halos (Figure 1). A positive

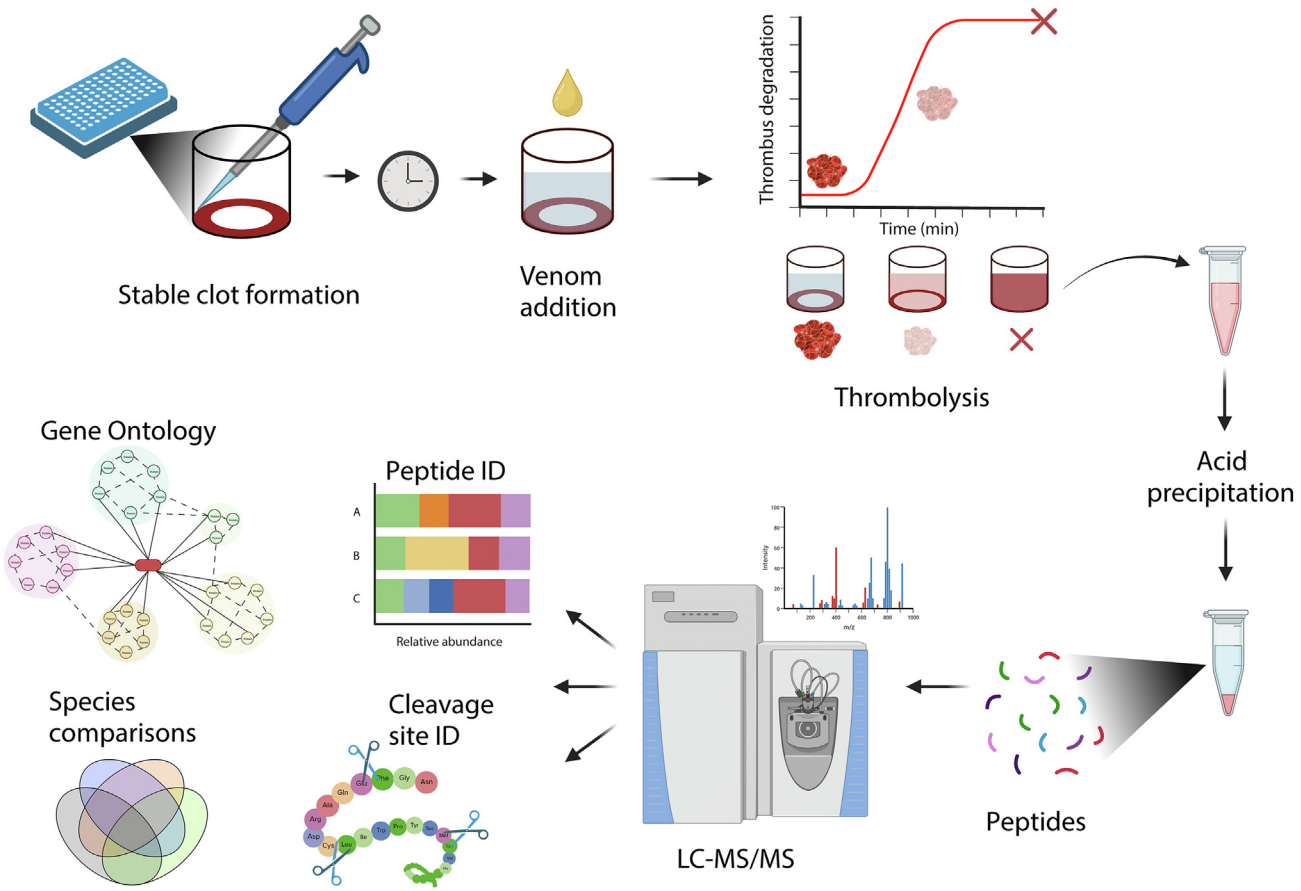

FIGURE 1 Halo thrombolytic assay and peptidomic analysis workflow. Whole blood clots are created in a 96-well plate. Snake venom or phosphate-buffered saline is added after 1 hour, and clot degradation is measured spectrophotometrically every minute for 2 hours. Supernatants from each well are removed, and degradation peptides were purified with perchloric acid precipitation for liquid chromatography-tandem mass spectrometry (LC-MS/MS) analysis. Blood clot degradation products were identified and compared across species to determine major cleavage site patterns, protein targets, and target functions.

control that lacked the clotting mixture was included. The plate was incubated for 1 hour at 37 °C to form stable clots.

Fibrinolysis was tested in triplicate with 6 different species of adult venomous snakes: *Bitis arietans* (BIAR), *Crotalus atrox* (southern Arizona; CRAT), *C. v. viridis* (northern Colorado; CRVI), *Dendroaspis viridis* (DEVI), *Naja savannula* (NASA), and *N. nigricollis* (NANI). Lyophilized venoms from CRAT and CRVI were obtained from snakes housed at the University of Northern Colorado (UNC) Animal Facility (Greeley, Colorado; Institutional Animal Care and Use Committee #2303D-SM-S-26). All other venoms were obtained from the Research Institute of Applied Biology of Guinea (Kindia, Guinea) from snakes captured in the region (IACUC #KJ062322). Venom was reconstituted at 4 mg/mL in double-distilled water and diluted into 70 μL phosphate-buffered saline (PBS) for a final concentration of 1 mg/mL, 100 μg/mL, or 10 μg/mL. Human plasmin diluted into PBS (0.01 U/mL, 0.3 U/mL, and 0.5 U/mL final concentration) was used as a positive control for fibrinolysis. Seventy microliters of PBS + venom, PBS + plasmin, or PBS alone (negative control) was added in triplicate simultaneously into the wells containing the clots.

Clot degradation was measured every minute over 2 hours with a Tecan Spark microplate reader by measuring absorbance change at 510 nm as previously described [31] (Figure 1). Before each absorbance reading, the plate was orbitally shaken for 5 seconds at 180 rpm with a 3 mm amplitude. The percentage of degradation was calculated as previously described [31] by subtracting the negative control value and normalizing absorbances to the positive control. Positive controls (containing no clotting mixture) represented full degradation, and negative controls (containing clotting mixture + PBS with no venom or plasmin) represented no fibrinolysis. The maximum clot lysis rate (CLR_{max}) was determined by calculating the first derivative of degradation profiles in GraphPad Prism 10. The time elapsed until 50% lysis (T0.5) and the area under the curve (AUC) was also calculated based on the degradation curves generated in Prism.

2.2 | Nano liquid chromatography-tandem mass spectrometry (LC-MS/MS)

Fifty micrograms of venom was digested with trypsin for shotgun proteomics analysis as previously described [32], and digested peptides were purified with Pierce C_{18} Spin Tips (Thermo Scientific)

according to the manufacturer's protocol. Samples were dried in a speed vacuum and redissolved in 0.1% formic acid (FA). LC-MS/MS was performed using an Easy nLC 1000 instrument coupled with a Q-Exactive HF Mass Spectrometer (both from ThermoFisher Scientific). Approximately 3 μg of digested peptides were loaded on a C_{18} column (100 μm inner diameter × 20 cm) packed in-house with 2.7 μm Cortecs C_{18} resin and separated at a flow rate of 0.4 μL/min with solution A (0.1% FA) and solution B (0.1% FA in acetonitrile) under the following conditions: isocratic at 4% B for 3 minutes, followed by 4% to 32% B for 102 minutes, 32% to 55% B for 5 minutes, 55% to 95% B for 1 minute, and isocratic at 95% B for 9 minutes. MS was performed in data-dependent acquisition mode. Full MS scans were obtained from m/z 300 to 1800 at a resolution of 60 000, an automatic gain control target of 1×10^6, and a maximum injection time of 50 m/s. The top 15 most abundant ions with an intensity threshold of 9.1×10^3 were selected for MS/MS acquisition at a 15 000 resolution, 1×10^5 automatic gain control, and a maximal injection time of 110 m/s. The isolation window was set to 2.0 m/z, and ions were fragmented at a normalized collision energy of 30. Dynamic exclusion was set to 20 seconds.

2.3 | Analysis of mass spectrometry data

Fragmentation spectra were interpreted against an in-house protein sequence database generated from the venom gland transcriptome of each species as previously described [33] using MSFragger within the FragPipe computational platform [34,35]. Reverse decoys and contaminants were included in the search database. Cysteine carbamidomethylation was selected as a fixed modification, methionine oxidation was selected as a variable modification, and precursor–ion mass tolerance and fragment–ion mass tolerance were set at 20 ppm and 0.4 Da, respectively. Fully tryptic peptides with a maximum of 2 missed tryptic cleavages were allowed, and the protein-level false discovery rate (FDR) was set to <1%. Identified proteins were classified by major venom toxin family, and their relative abundances were compared across samples using a sum-normalized total spectral intensity [36].

2.4 | Peptidomics

To capture the peptides released from lysed clots, the supernatant containing the products of clot degradation was removed from each well after the 2-hour thrombolysis incubation and centrifuged for 15 minutes at 4 °C and 18 000 *g*. The soluble material was removed from the pellet, and deproteinization with acid precipitation was performed on the supernatant. Four molar ice–cold perchloric acid was added to supernatants to a final concentration of 1 M and vortexed. Samples were incubated on ice for 5 minutes and centrifuged at 18 000 *g* for 2 minutes at 4 °C. Supernatant was transferred to new tubes, neutralized with ice–cold 2 M potassium hydroxide, vortexed, and pH was checked with pH paper to ensure samples were between 6.5 and 8.0 pH. Neutralized samples were spun at 18 000 *g* for 15 minutes at 4 °C again and supernatant collected. Peptides were purified with Pierce C_{18} Spin Tips (Thermo Scientific) according to the manufacturer's protocol, and LC-MS/MS was performed as described above using an Easy nLC 1000 instrument coupled with a Q-Exactive HF Mass Spectrometer. Peptide spectra were interpreted against the UniProt human database (containing reverse decoys and contaminants) using MSFragger within FragPipe [34,35] as mentioned above. Protease specificity was set to nonspecific, and the FDR was set to <1%.

Species-level differences in clot degradomes were compared with principal component analysis in MetaboAnalyst 5.0 [37]. Peptidomic data and protein-level cleavage patterns were visualized using Peptigram [38]. Proteomic identification of cleavage site specificity and flanking amino acid specificity analyses were performed with WebPICS [39]. In order to assess the differences between targets of venoms that caused full thrombolysis and those that did not, partial least-squares discriminant analysis (PLS-DA) was performed with a variable importance in projection (VIP) plot, and a volcano plot was generated with a fold change threshold of 3 ($\log_2$FC 1.58) and a *P* value threshold of 0.05. These were used to identify specific protein targets that significantly differed between functional venom groups, as well as their overall contribution to group differences. To assess protein interactions and the overall functional importance of the identified group of proteins to thrombus formation and stability, these proteins were used to produce a protein network in STRING V12.0 (Global Biodata Coalition and ELIXIR), in which line weight indicates the strength of data support for protein–protein interactions and a minimum interaction score of 0.7. STRING protein network nodes were colored based on Reactome database categories.

3 | RESULTS

3.1 | Halo assay fibrinolysis profiles

Thrombolysis profiles were generally dose-dependent in both venom- and plasmin-treated clots (Figure 2A–G). At the high dose of plasmin, full degradation was reached by minute 42 (Figure 2G), but in BIAR and CRAT venom-treated clots (Figure 2A, B), full degradation was not reached until minute 73 in all replicates. The highest dose of CRVI venom approached 50% clot lysis after 2 hours (Figure 2C), and all elapid-treated clots showed minimal thrombolysis (Figure 2D–F). DEVI venom appeared to have no detectable thrombolytic activity (Figure 2F), and AUC, T0.5, and CLR_{max} could not be calculated for this species, so it was omitted from further analyses. The highest AUC values were found in clots treated with CRAT and BIAR venom when comparing species at any concentration (Figure 2H). The AUC in NASA and NANI venom-treated clots were negligible compared with viperid values. However, CRVI venom-treated clots had a significantly lower AUC than BIAR and CRAT venom-treated clots. Plasmin-treated clots reached 50% degradation at 9.3 ± 3.5 minutes (Figure 2I)

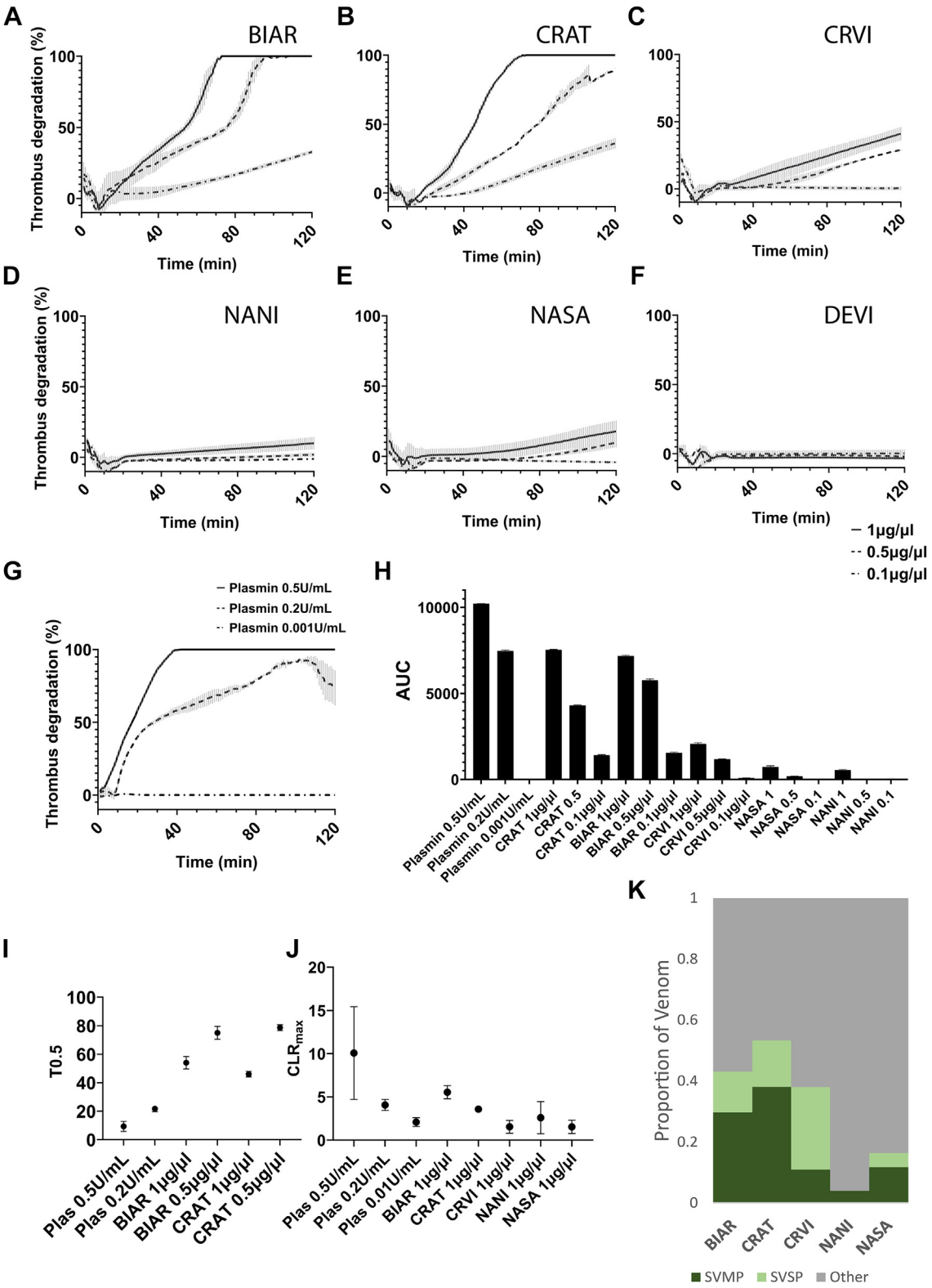

FIGURE 2 Snake venom thrombolytic profiles. Thrombolysis profiles of clots treated with venom at 1 µg/µL, 0.5 µg/µL, and 0.1 µg/µL from (A) *B. arietans* (BIAR), (B) *C. atrox* (CRAT), (C) *C. v. viridis* (CRVI), (D) *N. nigricollis* (NANI), (E) *N. savannula* (NASA), and (F) *D. viridis* (DEVI). (G) Thrombolysis profile of clots treated with plasmin at 0.5 U/mL, 0.2 U/mL, and 0.001 U/mL. (H) Area under the curve (AUC) comparisons of thrombolytic profiles between species and across concentrations represented as mean ± SD. (I) Time to 50% lysis (T0.5) comparisons for all treatments that reached at least 50% lysis. (J) Maximal clot lysis rates (CLR_{max}) comparing the highest concentration of venom (1 µg/µL) used for all species to all 3 concentrations of plasmin (Plas). (K) Shotgun proteomic data of venoms comparing relative abundance across species of the proteolytic enzymes snake venom metalloproteases (SVMPs) and snake venom serine proteases (SVSPs) to all other toxin families.

significantly faster than clots treated with even the most degradative snake venoms, BIAR and CRAT (54 ± 4.4 and 46 ± 2 minutes, respectively; $P < .0001$). Both BIAR and CRAT venom-treated clots reached 50% lysis at the highest dose (1 μg/μL), significantly faster than the middle dose (0.5 μg/μL; BIAR 54± 4.3 minutes vs 75 ± 4.6 minutes; CRAT 46± 2 minutes vs 78.7 ± 2.1 minutes; $P < .0001$). The CLR_{max} value of the highest dose of plasmin was significantly higher than the highest dose of all venoms, except for BIAR ($P = .20$; Figure 2J). While CLR_{max} did not differ between the highest doses of any venom, the highest value was found in the maximum dose of BIAR venom (5.5 ± 0.76 min^{-1}), and the lowest value was from NASA venome (1.5 ± 0.77 min^{-1}).

3.2 | Venom composition

Venom toxins identified by LC-MS/MS were grouped into major toxin families and further categorized as 1 of 2 major venom proteases (SVSP, SVMP) or as other for all nonproteolytic enzymes and all nonenzymatic toxins. The highest proportions of proteases belonged to the vipers, with BIAR and CRAT having the highest abundances of SVMPs and CRVI with the highest SVSP abundance (Figure 2K). NANI and NASA had overall lower levels of venom proteases, although NASA SVMP abundance was similar to that of CRVI.

3.3 | Protein and peptide identification

The number of peptides identified from degraded clots ranged from 0 in clots incubated with DEVI venom to 2810 peptides in clots incubated with BIAR venom. The highest number of peptides identified came from clots incubated with the venom of the 2 vipers that produced the highest rates of thrombolysis in the halo assay (2810 from BIAR and 2293 from CRAT; Figure 3A), and the lowest number of peptides resulted from incubation of clots with CRVI venom (1364 peptides). This was mirrored by the total number of identified clot proteins, with the highest number of proteins identified in BIAR (Figure 3B; 170 proteins) and CRAT (130 proteins) venom-treated clots and the lowest in CRVI venom-treated clots (75 proteins). On average, thrombi incubated with viper venoms (BIAR, CRAT, and CRVI) produced more than twice the number of clot-based peptides (2156 vs 1002 peptides; Figure 3C) and proteins (125 vs 68 proteins; Figure 3C) than those incubated with elapid venoms (NASA and NANI). Diversity values were calculated as the amount of cleavages/number of proteins. Interestingly, CRVI venom had the highest diversity value (36; Figure 3E), while NANI venom had the lowest diversity value [26].

There were 110 peptide degradation products mapping to 54 proteins common to all species (Figures 3F, G; Supplementary Table S1). Again, clots treated with BIAR venom produced the highest number of unique peptides and proteins (1372 unique peptides mapping to 34 proteins), while the lowest number of unique peptides and proteins (332 and 2, respectively) came from clots incubated with CRVI venom. Although many identified targets were shared between some or all species (Figure 3F), the abundances of these targets varied widely between species (Supplementary Table S2). When PLS-DA was performed comparing all species' degradomes separately, the abundances of hemoglobin subunit beta, alpha−1-antitrypsin, and fibrinogen alpha contributed the most to differentiating all 5 degradome profiles (Supplementary Figure S1, Supplementary Table S3).

Principal component analysis showed overall tight, consistent clustering of triplicates within species (Figure 3H). Replicates incubated with the 2 most thrombolytic venoms, BIAR and CRAT, clustered more closely together than with other species, while CRVI and NANI venoms formed another distinct cluster.

3.4 | Fibrin cleavage profiles

All venoms produced more cleavage products of fibrin chain alpha than of beta or gamma, and CRAT and BIAR clot degradomes showed the highest coverage/number of fibrin peptides detected overall (Figure 4A). All venoms produced degradation products associated with the cleavage of fibrinopeptide A (residues 20-35) and regions between residues 500 and 600 spanning the α connector (C) domain of the main fibrin alpha chain (Figure 4B; Supplementary Figure S2). Clots treated with CRAT and BIAR venoms also demonstrated high coverage and depth of chain alpha peptides in the αC region between residues 200 and 400. The highest intensities came from the αC peptides ^{223}LIKMKPVPDLVPGN^{236} and ^{393}FRPDSPGSGNARPNNPDWGT^{412} in CRAT venom-treated clots and ^{225}KPVPDLVPGN^{236} in BIAR venom-treated clots (Supplementary Figure S2). We identified the thrombin cleavage site at residues 35/36 across species and found degradation peptides flanking plasmin cleavage sites at residues 100 to 101 and 123 to 124 in BIAR and CRAT venom-treated clots only. We also identified a high number of fibrin alpha chain peptides flanking cross-linking sites at residues 322, 347, and 385 in BIAR and CRAT venom-treated clots, while all venoms produced degradation peptides flanking cross-linking sites at residues 527, 558, 575, 581, and 599.

Relative to the alpha chain, fibrin beta cleavage was significantly lower in all clot degradomes but was particularly low in CRVI, NANI, and NASA degradomes (Figure 4C) [38]. BIAR and CRAT degradomes showed the areas of highest peptide coverage between residues 58 to 72 of the main beta chain and another area between residues 150 and 163 that was absent in all other species, where 2 plasmin cleavage sites are found (Supplementary Figure S3). Fibrinopeptide B (residues 31-44) was found liberated from all clots except for CRVI venom-treated clots. This cleavage event is likely due to endogenous thrombin activity during thrombus formation. The peptide ^{58}SLRPAPPPISGGGYR^{72} had the highest intensity in BIAR and CRAT venom-treated clots, which is located downstream from a beta chain polymerization site at residues 45 to 47. Only BIAR and CRAT venoms produced degradation products of fibrin chain gamma from residues 66 to 109, which flank plasmin cleavage sites at residues 84/85 and

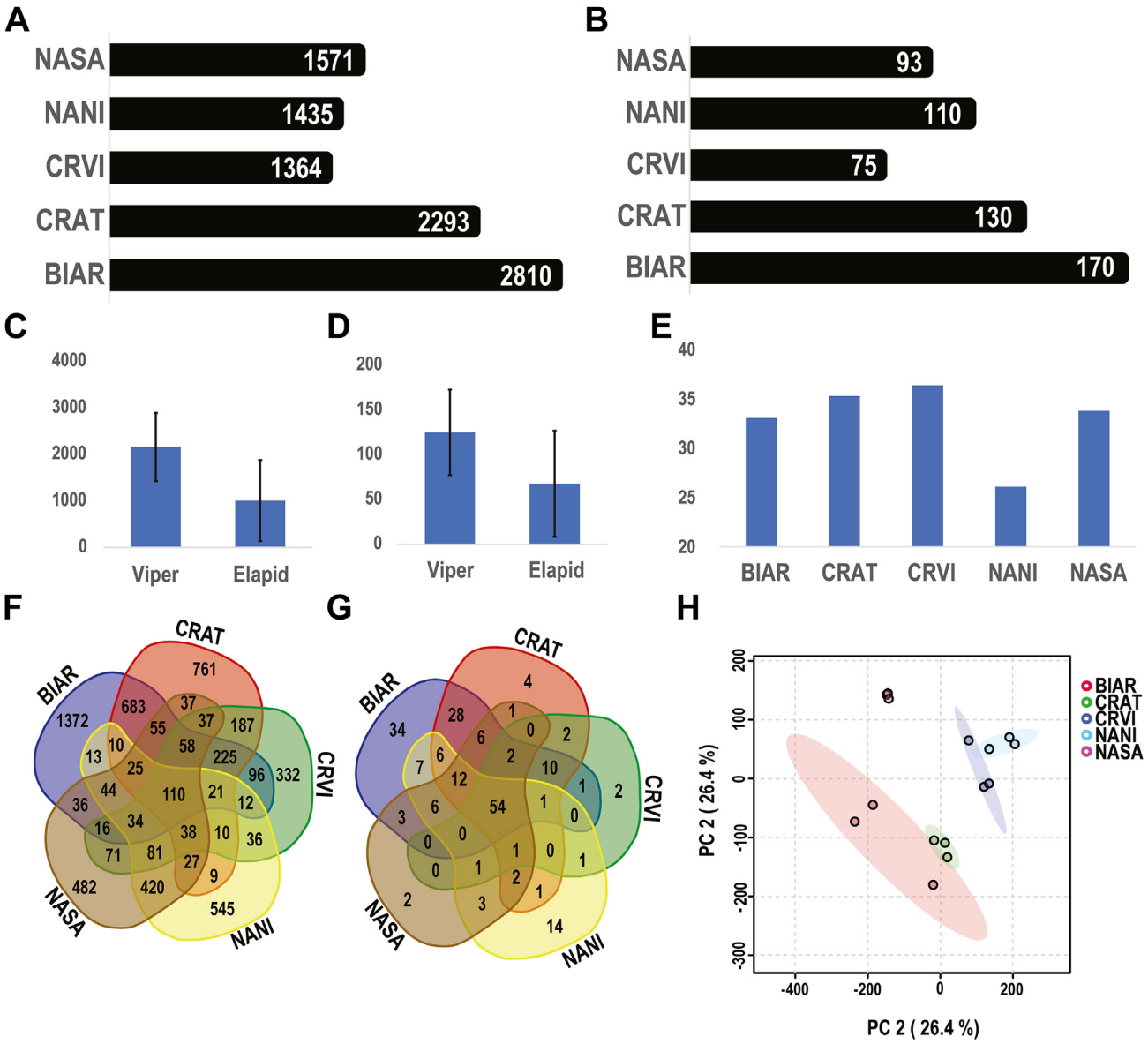

FIGURE 3 Peptide and protein identification of clot degradation products. The total number of unique (A) peptides and (B) proteins identified in venom-treated clots across species. Average number of (C) peptides and (D) proteins identified in clots treated with viper and elapid venoms. (E) Diversity values calculated as the number of cleavages/the number of proteins identified in clots. (F–G) Venn diagram showing the number of unique and shared degradome (F) peptides and (G) proteins across species. (H) Principal component analysis plot with 95% CIs of proteins identified in venom degradation profiles. BIAR, *B. arietans*; CRAT, *C. atrox*; CRVI, *C. v. viridis*; NANI, *N. nigricollis*; NASA, *N. savannula*.

88/89, and from residues 446 to the C-terminus (Figure 4D; Supplementary Figure S4). The C-terminal peptides identified in BIAR and CRAT clot degradomes are downstream of a fibrin alpha-gamma binding site, a gamma polymerization site at residues 400 to 422 and the platelet aggregation site at residues 423 to 437.

3.5 | Venom-wide cleavage sites

Fingerprints of cleavage specificity of the top 400 degradome peptides by intensity revealed differences in both snake family- and species-level cleavage residue preferences. Leucine at P1′ was favored in viper degradomes (Figures 4E–G), particularly in CRAT, but there was also a preference for leucine at P2′ for CRVI and P1 in BIAR. Viperid venoms also showed a preference for valine at P2′ (CRVI; Figure 4G) and P4 (BIAR; Figure 4E). BIAR and CRAT venoms showed a preference for proline in the P4′-P6′ region (Figure 4E, F). Last, BIAR venom showed a strong preference for glycine at P2′ (Figure 4E), and CRVI venom showed a preference for serine at P6′ (Figure 4G). NASA and NANI venom-induced cleavage events demonstrated a preference for aspartic acid at P1′ and a preference for leucine from P1 to P2′ of NASA (Figure 4H, I).

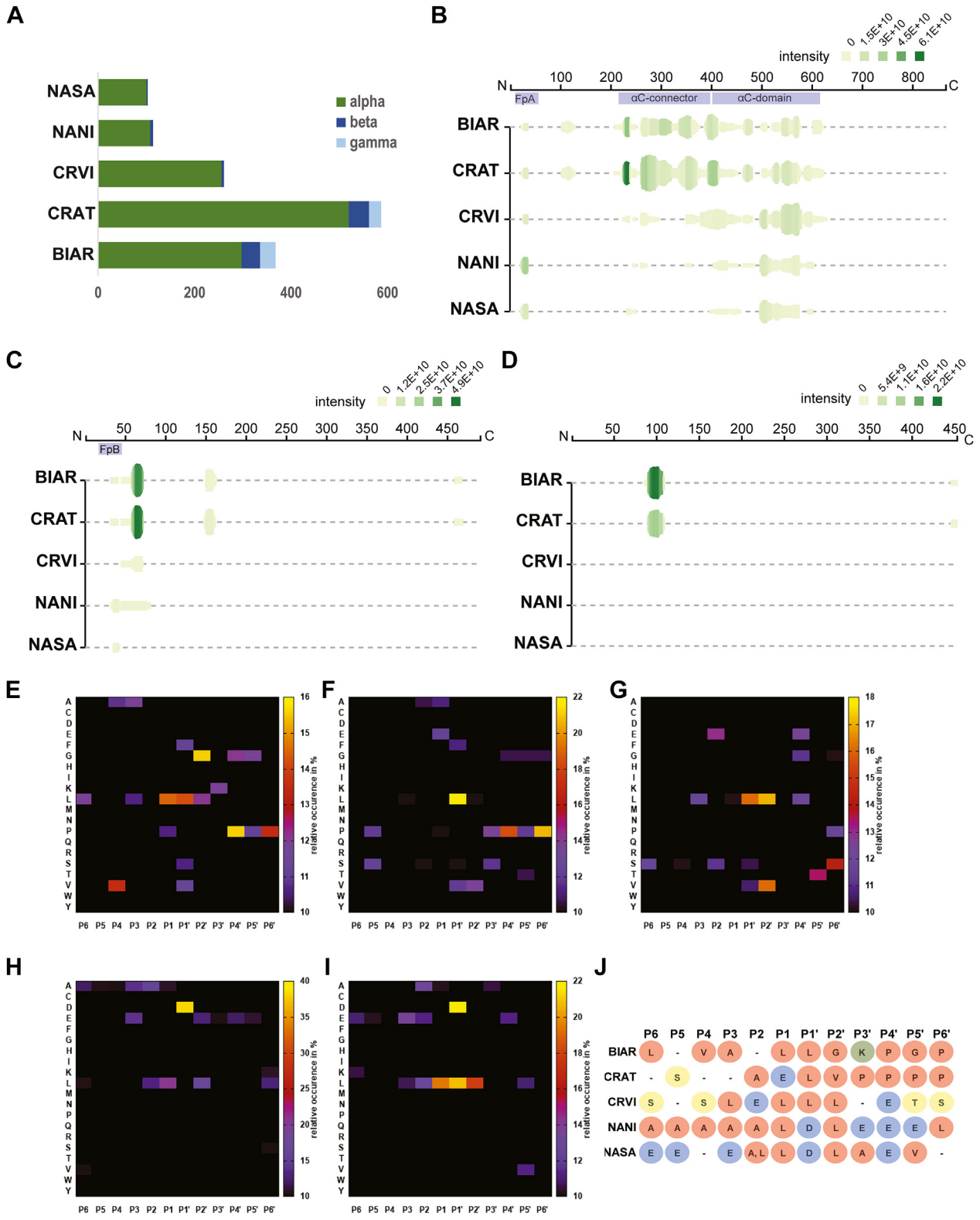

FIGURE 4 Peptidomic analysis of fibrin chain degradation and overall cleavage specificity. (A) Number of unique degradome peptides belonging to the alpha, beta, or gamma chains of fibrin. Peptide cleavage patterns of fibrin chain (B) alpha, (C) beta, and (D) gamma represented with Peptigram [38]. The plot height represents the number of overlapping peptides at a position, and the color represents the sum of the intensities (the total intensity for chromatographic peaks [area under the curve] corresponding to a detected peptide ion) of the overlapping peptides. Heatmap of the relative occurrence (in percentage) of each amino acid residue flanking cleavage sites among the top 400 most abundant peptides identified from clots treated with (E) BIAR (*B. arietans*), (F) CRAT (*C. atrox*), (G) CRVI (*C. v. viridis*), (H) NANI (*N. nigricollis*), and (I) NASA (*N. savannula*) venoms. (J) Most preferred residue at each position from P6-P6′ for each species.

We determined consensus preferences at each site from P6 to P6′ for each venom (Figure 4J). In general, we noted a strong preference for hydrophobic residues across flanking sites for all species, with a particular preference for leucine at P1 in all species but CRAT. We also noted the higher preference for acidic residues aspartic acid and glutamic acid in both elapid species and a preference for polar neutral residues in flanking regions in CRVI.

3.6 | Differences between venoms with varying levels of thrombolytic activity

To identify the major defining characteristics between strongly thrombolytic and minorly thrombolytic venoms we created a volcano plot and performed PLS-DA to identify clot degradation products that significantly differed in abundance that might define the 2 groups. The volcano plot showed BIAR and CRAT clot degradomes produced significantly higher abundance of 74 proteins including tubulin alpha 1B chain (TUBA1B), fibrinogen beta and gamma chains (FGB and FGG), N-acetylmuramoyl-L-alanine amidase (PGLYRP2), vitronectin (VTN), extracellular matrix protein 1 (ECM1), inter–alpha-trypsin inhibitor heavy chain H1 (ITIH1), hemoglobin subunit delta (HBD), pleckstrin (PLEK), and FN1 as major outliers (Figure 5A; Supplementary Table S4). The PLS-DA VIP plot demonstrated that the top 3 components with the highest VIP scores included alpha–1-antitrypsin (SERPINA1), hemoglobin subunit beta (HBB), and fibrinogen alpha (FGA; Figure 5B). The top 15 VIP scores also included FGB, alpha2–HS-glycoprotein (AHSG), glyceraldehyde-3-phosphate dehydrogenase (GAPDH), VTN, FGG, ITIH1, and alpha-synuclein (SNCA; Figure 5B; Supplementary Table S5). This demonstrates that the degradation of all 3 fibrin strands, in addition to other proteins that may be bound to clots, is a defining characteristic of highly thrombolytic venoms.

A STRING V12.0 protein–protein interaction network of the degradation targets that were significantly higher in clots treated with thrombolytic venoms produced a network with 71 nodes and 103 edges (Figure 5C). Major gene ontology biological processes identified included blood coagulation (FDR = 2.01e-06), fibrinolysis (FDR = 9.1e-07), and fibrin clot formation (FDR = 2.99e-05). Although other major interrelated pathways were also significant, including platelet aggregation (FDR = 1.46e-05), defense response (FDR = 2.37e-06), regulation of catalytic activity (FDR = 0.0084), and inflammatory response (FDR = 0.00092). The nodes with the highest degree of connectivity were proteins associated with clots or directly involved in clot architecture and stability including FN1 (n = 14), plasminogen (PLG; n = 13), apolipoprotein B-100 (APOB; n=11), FGA (n = 11), and FGB (n = 11).

4 | DISCUSSION

The amalgamation of functional thrombolytic assays and snake venom blood clot degradomes provides a complete framework of the proteolytic targets responsible for venom-induced thrombolysis. This has broad applications for the development of blood disorder therapeutics, snakebite treatment, and hematologic research tools. Here, we demonstrated the utility of a high-throughput halo assay in the quantification of venom-induced clot degradation and compared thrombolytic activities across 5 snakes with varied venom composition. Clot lysis rates were related to the abundance of SVMPs in each venom and their variable cleavage patterns toward clot-bound proteins. The high abundance of proteolytic toxins and their ability to target both cross-linking, cell adhesion, and plasmin cleavage sites of fibrin, as well as structurally pivotal clot-bound proteins, are consistent with the high thrombolytic activity of BIAR and CRAT venoms. Ultimately, this study expands our understanding of the thrombolytic and fibrinolytic effects of snake venom by determining the full suite of clot-specific venom targets that are involved in clot formation and stability.

We identified many of the same proteins in the clot degradome that were previously identified as either venom protease targets or as effector proteins in biofluids or tissues, including coagulation cascade factors, serpins, apolipoproteins, complement factors, ECM proteins, and fibrinogen chains [14,16,40] (Figure 6). Taken together, changes in the abundance of these endogenous proteins affect a wide variety of physiological responses to envenomation, including thromboinflammation, immune system activation, hemostatic alterations, and cell and tissue destruction [14–17,40–42] (Supplementary Table S6). However, correlating the differences in protein abundance and degradation products of envenomated tissues with measurable differences in biological and physiological functions presents a significant challenge. To understand how some of these venom targets relate to clot degradation, we focused specifically on integrating the observed differences in clot degradome peptides with the measurable differences in thrombolytic activity between snake venoms.

Vipers are generally known to produce highly proteolytic venom compared with elapids [43,44]. In this study, the 3 vipers demonstrated much higher overall protease abundance than the elapids; however, only the venoms of 2 SVMP-rich viper species, BIAR and CRAT, were able to initiate full thrombolysis after 2 hours. Even the low-protease venoms produced some proteolytic activity against fibrin alpha and beta chains and other clot-stabilizing proteins, suggesting that the higher rates of thrombolysis in CRAT and BIAR are, unsurprisingly and at least in part, dependent on the higher abundance of metalloproteases in their venoms.

The generation of venom-induced cleavage fingerprints provides key new perspectives on the combined cleavage patterns induced by venom toxins, which has the potential to reveal both novel patterns of proteolysis and strengthen the ability to predict other unexplored substrates. Species showed characteristic differences in cleavage site preferences indicative of an overall divergence in activities between active proteases in each venom. Despite using crude venom, proteolytic signatures resulting from the action of highly abundant SVMPs in viperid venoms were still detectable. For example, we detected the previously noted preference for Leu at P1′ of SVMPs (and metalloproteases in general) in all 3 viper venoms [14–16].

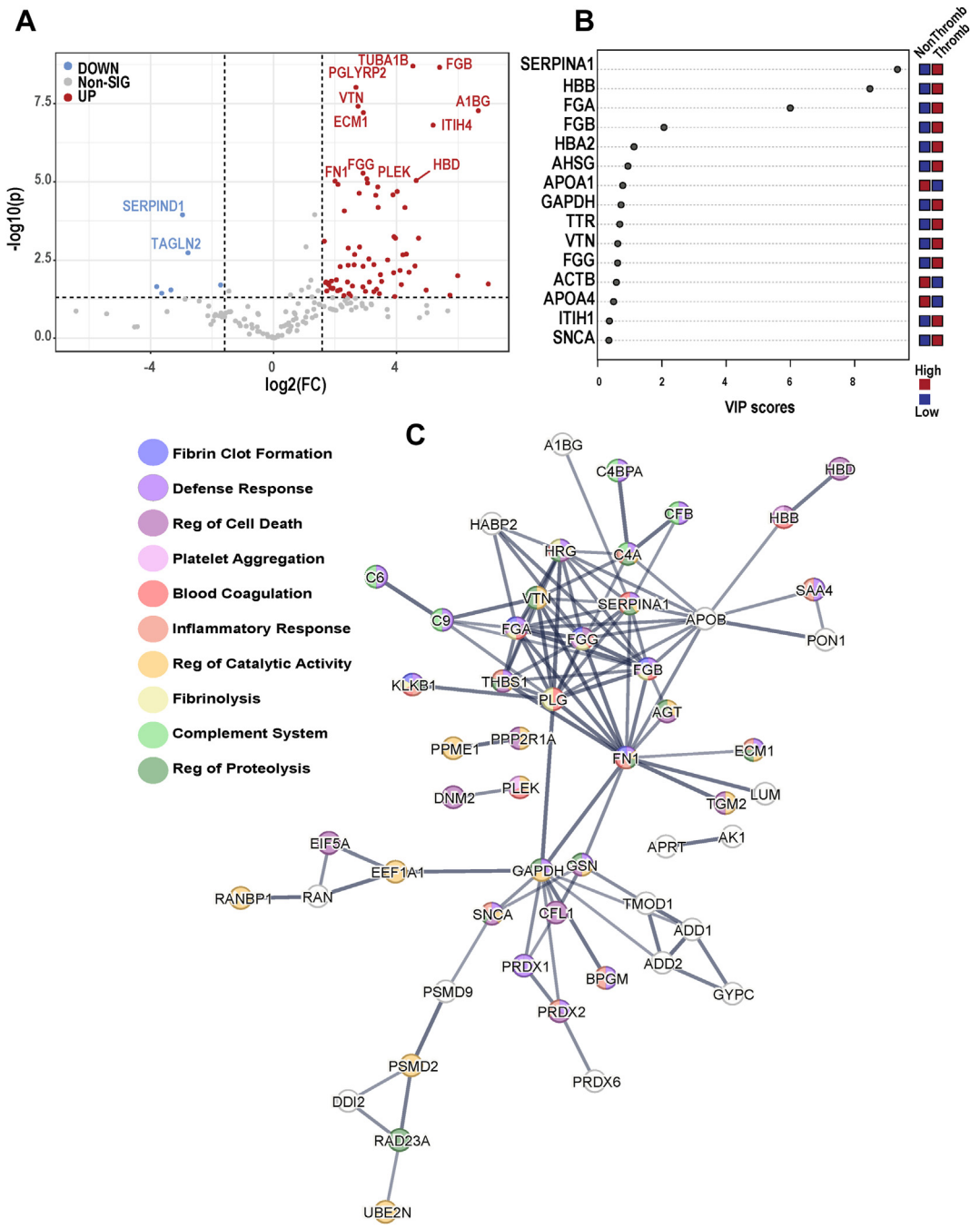

FIGURE 5 Defining features of thrombolytic venom degradomes. (A) Volcano plot comparing differences in protein abundance between clots incubated with thrombolytic venoms that reached 100% thrombus degradation (BIAR [*B. arietans*] and CRAT [*C. atrox*]) and less thrombolytic venoms that did not reach 50% degradation after 2 hours. (B) Variable importance in projection (VIP) scores of the 15 most important degradome proteins in partial least-squares discriminant analysis distinguishing thrombolytic from less thrombolytic venoms. Red indicates the group that had a significantly higher abundance of the specified protein in the degradome, and blue indicates the group that had a significantly lower abundance of the specified protein in the degradome. (C) STRING V12.0 protein interaction network with overlaid gene ontology analysis of proteins identified as significantly higher in the degradomes of thrombolytic venoms.

The cleavage of fibrin(ogen) chains alpha, beta, and gamma by various venom proteases has repeatedly been observed [14]. Using Peptigram software, we characterized the unique protein cleavage patterns for all 3 fibrin(ogen) chains, noting enhanced proteolytic activity and broader coverage across all chains for BIAR and CRAT venoms compared with all other species. We also noted that the most thrombolytic venoms targeted fibrin regions essential for clot stability, including regions involved in cross-linking, fibrinolysis inhibition, and cell adhesion.

Alpha chain cross-links throughout the αC domains are integral to fibrin polymer assembly [45]. We found extensive degradation across alpha chain interchain binding sites, particularly by BIAR and CRAT

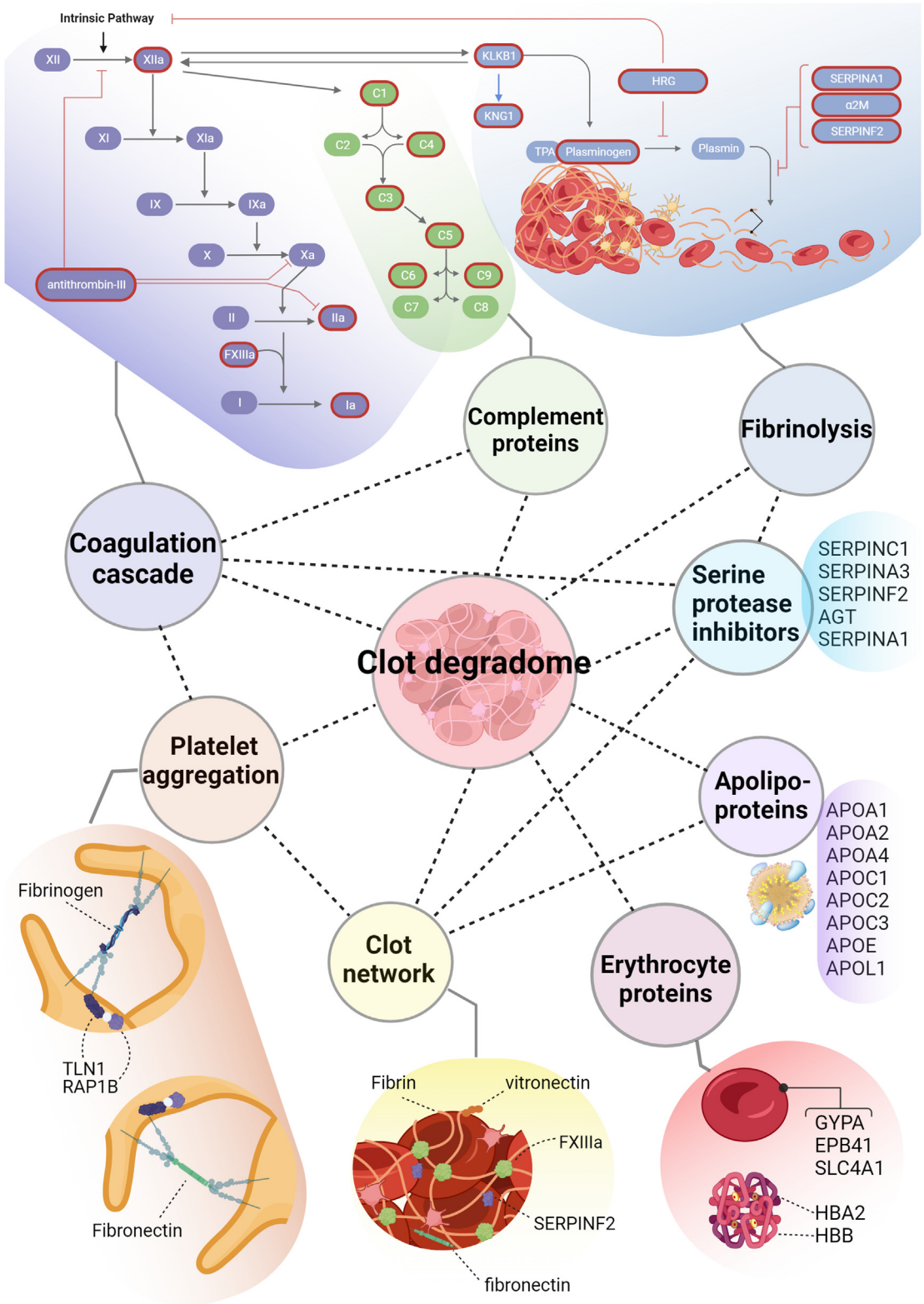

FIGURE 6 Snake venom clot degradome. Simplified gene ontology network with proteins identified in the snake venom blood clot degradome created with BioRender (Biorender.com). Protein targets associated with the coagulation cascade, complement system, and fibrinolysis are circled in red, and all other targets are listed in black.

venoms, with a high number of peptides originating from the αC domain, indicating possible compromise of alpha cross-links and therefore clot stiffness and elasticity. BIAR and CRAT venoms also recognized multiple cleavage sites at or flanking plasmin cleavage sites in the alpha and beta chains. This plasmin-like activity is likely unrelated to endogenous plasmin activity, as we did not detect peptides

associated with plasminogen activation. These thrombolytic venoms also uniquely targeted residues flanking the alpha–2-antiplasmin binding site of chain alpha, possibly neutralizing the protective effects against fibrinolysis of this protein. BIAR and CRAT venom-treated clots showed significantly higher degradation of fibrin chain beta, particularly in the beta chain polymerization site toward the N-terminal where binding to the distal site of another fibrin strand occurs.

The gamma chain of fibrin is pivotal to the formation of structurally sound fibrin polymers with high mechanical resistance, and polymers lacking gamma chain cross-links produce unstable clots that easily fragment [46]. The gamma chain also accelerates thrombin-mediated factor XIII (FXIII) activation, thereby enhancing clot stability facilitated by FXIIIa activity. We specifically noted cleavage by BIAR and CRAT venoms of the C-terminal portion of fibrin chain gamma [14], the region involved in fibrin stabilization via cross-links [47], and platelet interactions via integrin binding [48,49]. As platelet aggregation is another critical step in clot formation, the targeting of this region by CRAT and BIAR venoms likely plays a significant role in thrombolysis by compromising the stiffness and structure of the fibrin network and by interfering with platelet aggregation in stable clots.

Coagulation FXIIIa is critical for clot stabilization during coagulation via its catalysis of fibrin cross-links and of cross-linking of fibrin to other proteins including alpha–2-antiplasmin [50,51], inter–alpha-inhibitor [52], FN1, HRG [53], ECM-1, alpha–2-macroglobulin, plasminogen, and c3 [54]. We identified cleavage of FXIII A subunit in all venoms, which remains associated with the clot after the active B subunit is released [55], as well as downstream degradation products of FXIIIa from the clot degradomes of BIAR and CRAT.

Enzyme-rich thrombolytic venoms also demonstrated increased activity toward other clot-stabilizing proteins that are substrates of FXIIIa [51], including FN1, VTN, ECM-1, and lumican [14,17,18]. FN1 covalently cross-links to fibrin to significantly increase clot stability and size [56], and association with FN1 specifically has been shown to increase the adhesive properties of fibrin, making FN1 critical for clot retention of stabilizing platelets and other cellular material [57]. We noted cleavage sites flanking cell attachment and Fibulin-1 (FBLN1) binding sites of fibronectin in the clot degradome of multiple species, but only BIAR and CRAT clot degradomes showed peptides from the N-terminal region of fibrin-binding site 2. Therefore, venom may compromise the stabilizing properties of FN1-mediated cell and platelet adhesion to clots by degrading both FN1 sites of cell adhesion and interfering with fibrin-FN1 interactions.

VTN is known to inhibit fibrinolysis by complexing with type 1 plasminogen activator inhibitor on fibrin polymers [58]. Further, VTN preferentially binds to the carboxyl-terminal of the gamma chain of fibrin, another venom target discussed above involved in clot stabilization via cross-linking [59]. VTN-deficient thrombi are inherently unstable and show an increased tendency to embolize [59,60]. BIAR and CRAT clot profiles had the highest number of peptides resulting from VTN degradation, and we noted peptides that spanned the RGD cell attachment site of VTN in NASA, CRVI, and CRAT clot profiles, suggesting further interference with structural protein-mediated cell adhesion.

The clot-stabilizing proteins and fibrin chains discussed above support clot architecture by altering the physical properties of a thrombus, including its permeability, resistance to lysis, clot stiffness, and cell-adhesive properties [45,57]. A comprehensive understanding of how these proteins interact to regulate thrombus formation, structure, and stability is pivotal for identifying novel targets for future anticoagulant and thrombolytic therapies [61]. Measurable structural differences in clot architecture caused by deficiencies or enrichment in specific clot-bound proteins can be detected in proteomic clot profiles and correlated with various disease states and clinical outcomes [62–64]. This allows for the identification of specific therapeutic targets [65].

Though snake venoms are toxic mixtures with a wide array of biological effects, some proteins are pharmacologically active but nontoxic when isolated [66]. Numerous snake venom toxins have already been identified for their therapeutic utility in the treatment of coagulopathies [67,68], For example, eptifibatide, a drug designed from the structure of a peptide derived from *Sistrurus miliarius barbouri* venom, is used to treat acute coronary syndrome due to its effects on platelet aggregation [69]. Further, venom proteins specifically have shown utility as diagnostic research tools in the study of hemostatic disorders [8]. For example, venom enzymes that activate coagulation factors or other plasma proteins [70,71] have been used to test for specific protein levels in blood and to elucidate the mechanisms behind the coagulation cascade [8]. Therefore, cataloging the entire suite of toxin targets in blood clots and the resulting functional effect of their cleavage has tremendous implications for the bioprospecting of thrombolytic therapies. Ultimately, our data adds to the repertoire of snake venom hematological targets and provides a holistic picture of the molecular basis of thrombolysis catalyzed by snake venoms, paving the way for further investigation of hemostatic alterations triggered by venom toxins using omics technologies.

AUTHOR CONTRIBUTIONS

C.F.S. performed field work, collected venom samples, designed and performed experiments, processed and analyzed data, and wrote the manuscript. M.A.B., M.M., N.C., J.B., N.P.B., C.B., and K.J. performed field work, collected venom samples, and edited the manuscript. S.F. and C.M.M. compiled the transcriptome-guided venom databases and edited the manuscript. L.B., M.A.A., K.Y.L., S.P.M., and D.C.G. performed lab work, sample preparation, and mass spectrometry runs. M.M. and M.J.C. edited the manuscript and provided assistance with mass spectrometry method design and provided clinical expertise, respectively. T.A.C., S.P.M., and K.C.H. contributed to study design, data interpretation, and edited the manuscript. A.J.S. designed experiments, analyzed data, and assisted with writing and editing the manuscript. All authors read and approved the final version of this manuscript.

DECLARATION OF COMPETING INTERESTS

There are no competing interests to disclose.

DATA AVAILABILITY

The raw peptidomic data used for this study are available upon request to the corresponding author, A.J.S.

ORCID

Cara F. Smith https://orcid.org/0000-0002-6868-7713
Todd A. Castoe https://orcid.org/0000-0002-5912-1574
Stephen P. Mackessy https://orcid.org/0000-0003-4515-2545
Kirk C. Hansen https://orcid.org/0000-0001-5054-838X
Anthony J. Saviola https://orcid.org/0000-0001-6890-512X

REFERENCES

[1] Swenson S, Markland FS. Snake venom fibrin(ogen)olytic enzymes. *Toxicon*. 2005;45:1021–39.
[2] Sanchez EF, Flores–Ortiz RJ, Alvarenga VG, Eble JA. Direct fibrinolytic snake venom metalloproteinases affecting hemostasis: structural, biochemical features and therapeutic potential. *Toxins (Basel)*. 2017;9:392.
[3] Kalita B, Saviola AJ, Samuel SP, Mukherjee AK. State-of-the-art review - A review on snake venom-derived antithrombotics: potential therapeutics for COVID–19-associated thrombosis? *Int J Biol Macromol*. 2021;192:1040–57.
[4] Marsh N, Williams V. Practical applications of snake venom toxins in haemostasis. *Toxicon*. 2005;45:1171–81.
[5] White J. Snake venoms and coagulopathy. *Toxicon*. 2005;45:951–67.
[6] McCleary RJR, Kini RM. Snake bites and hemostasis/thrombosis. *Thromb Res*. 2013;132:642–6.
[7] Jeon YJ, Kim JW, Park SG, Shin DW. Risk factor, monitoring, and treatment for snakebite induced coagulopathy: a multicenter retrospective study. *Acute Crit Care*. 2019;34:269–75.
[8] Moore GW. Snake venoms in diagnostic hemostasis and thrombosis. *Semin Thromb Hemost*. 2022;48:145–60.
[9] Xiong S, Huang C. Synergistic strategies of predominant toxins in snake venoms. *Toxicol Lett*. 2018;287:142–54.
[10] Laustsen AH. Toxin synergism in snake venoms. *Toxin Rev*. 2016;35:165–70.
[11] Escalante T, Rucavado A, Fox JW, Gutiérrez JM. Key events in microvascular damage induced by snake venom hemorrhagic metalloproteinases. *J Proteomics*. 2011;74:1781–94.
[12] Kini RM, Koh CY. Metalloproteases affecting blood coagulation, fibrinolysis and platelet aggregation from snake venoms: definition and nomenclature of interaction sites. *Toxins (Basel)*. 2016;8:284.
[13] Kini RM. Serine proteases affecting blood coagulation and fibrinolysis from snake venoms. *Pathophysiol Haemost Thromb*. 2005;34:200–4.
[14] Bertholim L, Chaves AFA, Oliveira AK, Menezes MC, Asega AF, Tashima AK, Zelanis A, Serrano SMT. Systemic effects of hemorrhagic snake venom metalloproteinases: untargeted peptidomics to explore the pathodegradome of plasma proteins. *Toxins (Basel)*. 2021;13:764.
[15] Zelanis A, Oliveira AK, Prudova A, Huesgen PF, Tashima AK, Kizhakkedathu J, Overall CM, Serrano SMT. Deep profiling of the cleavage specificity and human substrates of snake venom metalloprotease HF3 by proteomic identification of cleavage site specificity (PICS) using proteome derived peptide libraries and terminal amine isotopic labeling of substrates (TAILS) N-terminomics. *J Proteome Res*. 2019;18:3419–28.
[16] Asega AF, Menezes MC, Trevisan-Silva D, Cajado-Carvalho D, Bertholim L, Oliveira AK, Zelanis A, Serrano SMT. Cleavage of proteoglycans, plasma proteins and the platelet-derived growth factor receptor in the hemorrhagic process induced by snake venom metalloproteinases. *Sci Rep*. 2020;10:12912. https://doi.org/10.1038/s41598-020-69396-y
[17] Paes Leme AF, Sherman NE, Smalley DM, Sizukusa LO, Oliveira AK, Menezes MC, Fox JW, Serrano SMT. Hemorrhagic activity of HF3, a snake venom metalloproteinase: insights from the proteomic analysis of mouse skin and blood plasma. *J Proteome Res*. 2012;11:279–91.
[18] Oliveira AK, Paes Leme AF, Asega AF, Camargo ACM, Fox JW, Serrano SMT. New insights into the structural elements involved in the skin haemorrhage induced by snake venom metalloproteinases. *Thromb Haemost*. 2010;104:485–97.
[19] Slagboom J, Kool J, Harrison RA, Casewell NR. Haemotoxic snake venoms: their functional activity, impact on snakebite victims and pharmaceutical promise. *Br J Haematol*. 2017;177:947–59.
[20] Isbister GK. Procoagulant snake toxins: laboratory studies, diagnosis, and understanding snakebite coagulopathy. *Semin Thromb Hemost*. 2009;35:93–103.
[21] Li S, Ji H, Cheng X, Li BXY, Ng TB. Antithrombotic and thrombolytic activities of Agkisacutacin, a snake venom proteinase, in experimental models. *Gen Pharmacol*. 2000;35:179–87.
[22] Alcachupas A, Bellosillo K, Catolico WR, Davis MC, Diaz A, Doyongan YK, Eduarte R, Gersava E, Intrepido MB, Laluma MGK, Lavalle CC, Millan J Jr. Thrombolytic effects of Philippine pit viper (Trimeresurus flavomaculatus) venom in human blood in vitro and ferric chloride-induced cardiac thrombosis on Swiss Webster mice in vivo. *Cureus*. 2023;15:e40856. https://doi.org/10.7759/cureus.40856
[23] Jacob–Ferreira AL, Menaldo DL, Bernardes CP, Sartim MA, De Angelis CD, Tanus–Santos JE, Sampaio SV. Evaluation of the *in vivo* thrombolytic activity of a metalloprotease from *Bothrops atrox* venom using a model of venous thrombosis. *Toxicon*. 2016;109:18–25.
[24] Pidde–Queiroz G, Magnoli FC, Portaro FCV, Serrano SMT, Lopes AS, Paes Leme AF, van den Berg CW, Tambourgi DV. P-I snake venom metalloproteinase is able to activate the complement system by direct cleavage of central components of the cascade. *PLoS Negl Trop Dis*. 2013;7:e2519. https://doi.org/10.1371/journal.pntd.0002519
[25] Kuppusamy M, Huesgen PF. 'Omics' approaches to determine protease degradomes in complex biological matrices. In: Zelanis A, ed. *Proteolytic Signaling in Health and Disease*. London, UK: Academic Press; 2021:209–28.
[26] Foreman RE, George AL, Reimann F, Gribble FM, Kay RG. Peptidomics: a review of clinical applications and methodologies. *J Proteome Res*. 2021;20:3782–97.
[27] Zhang HE, Hamson EJ, Koczorowska MM, Tholen S, Chowdhury S, Bailey CG, Lay AJ, Twigg SM, Lee Q, Roediger B, Biniossek ML, O'Rourke MB, McCaughan GW, Keane FM, Schilling O, Gorrell MD. Identification of novel natural substrates of fibroblast activation protein-alpha by differential degradomics and proteomics. *Mol Cell Proteomics*. 2019;18:65–85.
[28] Bsat S, Chanbour H, Bsat A, Alomari S, Moussalem C, El Houshiemy MN, Omeis I. Clinical utility of degradomics as predictors of complications and clinical outcome in aneurysmal subarachnoid hemorrhage. *J Integr Neurosci*. 2021;20:489–97.
[29] Latosinska A, Frantzi M, Siwy J. Peptides as "better biomarkers"? Value, challenges, and potential solutions to facilitate implementation. *Mass Spectrom Rev*. 2023;43:1195–236.
[30] Hellinger R, Sigurdsson A, Wu W, Romanova EV, Li L, Sweedler JV, Süssmuth RD, Gruber CW. Peptidomics. *Nat Rev Methods Primers*. 2023;3:25.

[31] Bonnard T, Law LS, Tennant Z, Hagemeyer CE. Development and validation of a high throughput whole blood thrombolysis plate assay. *Sci Rep*. 2017;7:2346.
[32] Grabowsky ER, Saviola AJ, Alvarado–Díaz J, Mascareñas AQ, Hansen KC, Yates JR, Mackessy SP. Montane Rattlesnakes in México: venoms of *Crotalus tancitarensis* and related species within the *Crotalus intermedius* group. *Toxins (Basel)*. 2023;15:72.
[33] Smith CF, Modahl CM, Galindo DC, Larson KY, Maroney SP, Bahrabadi L, Brandehoff NP, Perry BW, McCabe MC, Petras D, Lomonte B, Calvete JJ, Castoe TA, Mackessy SP, Hansen KC, Saviola AJ. Assessing target specificity of the small molecule inhibitor MARIMASTAT to snake venom toxins: a novel application of thermal proteome profiling. *Mol Cell Proteomics*. 2024;23:100779. https://doi.org/10.1016/j.mcpro.2024.100779
[34] Yu F, Teo GC, Kong AT, Haynes SE, Avtonomov DM, Geiszler DJ, Nesvizhskii AI. Identification of modified peptides using localization-aware open search. *Nat Commun*. 2020;11:4065. https://doi.org/10.1038/s41467-020-17921-y
[35] Kong AT, Leprevost FV, Avtonomov DM, Mellacheruvu D, Nesvizhskii AI. MSFragger: ultrafast and comprehensive peptide identification in mass spectrometry-based proteomics. *Nat Methods*. 2017;14:513–20.
[36] Zhu W, Smith JW, Huang CM. Mass spectrometry-based label-free quantitative proteomics. *J Biomed Biotechnol*. 2010;2010:840518. https://doi.org/10.1155/2010/840518
[37] Pang Z, Chong J, Zhou G, De Lima Morais DA, Chang L, Barrette M, Gauthier C, Jacques PÉ, Li S, Xia J. MetaboAnalyst 5.0: narrowing the gap between raw spectra and functional insights. *Nucleic Acids Res*. 2021;49:W388–96.
[38] Manguy J, Jehl P, Dillon ET, Davey NE, Shields DC, Holton TA. Peptigram: a web-based application for peptidomics data visualization. *J Proteome Res*. 2017;16:712–9.
[39] Schilling O, Overall CM. Proteome-derived, database-searchable peptide libraries for identifying protease cleavage sites. *Nat Biotechnol*. 2008;26:685–94.
[40] Trevisan–Silva D, Cosenza–Contreras M, Oliveira UC, da Rós N, Andrade–Silva D, Menezes MC, Oliveira AK, Rosa JG, Sachetto ATA, Biniossek ML, Pinter N, Santoro ML, Nishiyama MY Jr, Schilling O, Serrano SMT. Systemic toxicity of snake venom metalloproteinases: multi-omics analyses of kidney and blood plasma disturbances in a mouse model. *Int J Biol Macromol*. 2023;253:127279. https://doi.org/10.1016/j.ijbiomac.2023.127279
[41] Ahmadi S, Pachis ST, Kalogeropoulos K, McGeoghan F, Canbay V, Hall SR, Crittenden EP, Dawson CA, Bartlett KE, Gutiérrez JM, Casewell NR, Keller UAD, Laustsen AH. Proteomics and histological assessment of an organotypic model of human skin following exposure to *Naja nigricollis* venom. *Toxicon*. 2022;220:106955. https://doi.org/10.1016/j.toxicon.2022.106955
[42] Rucavado A, Escalante T, Shannon J, Gutiérrez JM, Fox JW. Proteomics of wound exudate in snake venom-induced pathology: search for biomarkers to assess tissue damage and therapeutic success. *J Proteome Res*. 2011;10:1987–2005.
[43] Tasoulis T, Isbister GK. A review and database of snake venom proteomes. *Toxins (Basel)*. 2017;9:290.
[44] Tasoulis T, Pukala TL, Isbister GK. Investigating toxin diversity and abundance in snake venom proteomes. *Front Pharmacol*. 2022;12:768015. https://doi.org/10.3389/fphar.2021.768015
[45] Helms CC, Ariëns RAS, Uitte De Willige S, Standeven KF, Guthold M. α–α Cross-links increase fibrin fiber elasticity and stiffness. *Biophys J*. 2012;102:168–75.
[46] Duval C, Baranauskas A, Feller T, Ali M, Cheah LT, Yuldasheva NY, Baker SR, McPherson HR, Raslan Z, Bailey MA, Cubbon RM, Connell SD, Ajjan RA, Philippou H, Naseem KM, Ridger VC, Ariëns RAS. Elimination of fibrin γ-chain cross-linking by FXIIIa increases pulmonary embolism arising from murine inferior vena cava thrombi. *Proc Natl Acad Sci U S A*. 2021;118:e2103226118. https://doi.org/10.1073/pnas.2103226118
[47] Chen R, Doolittle RF. Isolation, characterization, and location of a donor-acceptor unit from cross-linked fibrin. *Proc Natl Acad Sci U S A*. 1970;66:472–9.
[48] Springer TA, Zhu J, Xiao T. Structural basis for distinctive recognition of fibrinogen γC peptide by the platelet integrin $\alpha_{IIb}\beta_3$. *J Cell Biol*. 2008;182:791–800.
[49] Ware S, Donahue JP, Hawiger J, Anderson WF. Structure of the fibrinogen γ-chain integrin binding and factor XIIIa cross-linking sites obtained through carrier protein driven crystallization. *Protein Sci*. 1999;8:2663–71.
[50] Sakata Y, Aoki N. Significance of cross-linking of α_2-plasmin inhibitor to fibrin in inhibition of fibrinolysis and in hemostasis. *J Clin Invest*. 1982;69:536–42.
[51] Nikolajsen CL, Dyrlund TF, Poulsen ET, Enghild JJ, Scavenius C. Coagulation factor XIIIa substrates in human plasma: identification and incorporation into the clot. *J Biol Chem*. 2014;289:6526–34.
[52] Scavenius C, Sanggaard KW, Nikolajsen CL, Bak S, Valnickova Z, Thøgersen IB, Jensen ON, Højrup P, Enghild JJ. Human inter–α-inhibitor is a substrate for factor XIIIa and tissue transglutaminase. *Biochim Biophys Acta*. 2011;1814:1624–30.
[53] Halkier T, Andersen H, Vestergaard A, Magnusson S. Bovine histidine-rich glycoprotein is a substrate for bovine plasma factor XIIIa. *Biochem Biophys Res Commun*. 1994;200:78–82.
[54] Nikolajsen CL, Scavenius C, Enghild JJ. Human complement C3 is a substrate for transglutaminases. A functional link between non–protease-based members of the coagulation and complement cascades. *Biochemistry*. 2012;51:4735–42.
[55] Souri M, Osaki T, Ichinose A. The non–catalytic B subunit of coagulation factor XIII accelerates fibrin cross-linking. *J Biol Chem*. 2015;290:12027–39.
[56] Ni H, Yuen PST, Papalia JM, Trevithick JE, Sakai T, Fässler R, Jensen ON, Højrup P, Enghild JJ. Plasma fibronectin promotes thrombus growth and stability in injured arterioles. *Proc Natl Acad Sci U S A*. 2003;100:2415–9.
[57] Corbett SA, Lee L, Wilson CL, Schwarzbauer JE. Covalent cross-linking of fibronectin to fibrin is required for maximal cell adhesion to a fibronectin–fibrin matrix. *J Biol Chem*. 1997;272:24999–5005.
[58] Preissner KT, Holzhüter S, Justus C, Müller–Berghaus G. Identification of and partial characterization of platelet vitronectin: evidence for complex formation with platelet-derived plasminogen activator inhibitor-1. *Blood*. 1989;74:1989–96.
[59] Podor TJ, Campbell S, Chindemi P, Foulon DM, Farrell DH, Walton PD, Weitz JI, Peterson CB. Incorporation of vitronectin into fibrin clots. Evidence for a binding interaction between vitronectin and γA/γ′ fibrinogen. *J Biol Chem*. 2002;277:7520–8.
[60] Konstantinides S, Schäfer K, Thinnes T, Loskutoff DJ. Plasminogen activator inhibitor-1 and its cofactor vitronectin stabilize arterial thrombi after vascular injury in mice. *Circulation*. 2001;103:576–83.
[61] Howes JM, Keen JN, Findlay JBC, Carter AM. The application of proteomics technology to thrombosis research: the identification of potential therapeutic targets in cardiovascular disease. *Diab Vasc Dis Res*. 2008;5:205–12.
[62] Mihalko E, Brown AC. Clot structure and implications for bleeding and thrombosis. *Semin Thromb Hemost*. 2020;46:96–104.
[63] Muñoz R, Santamaría E, Rubio I, Ausín K, Ostolaza A, Labarga A, Roldán M, Zandio B, Mayor S, Bermejo R, Mendigaña M, Herrera M, Aymerich N, Olier J, Gállego J, Mendioroz M, Fernández-Irigoyen J. Mass spectrometry-based proteomic profiling of thrombotic

material obtained by endovascular thrombectomy in patients with ischemic stroke. *Int J Mol Sci*. 2018;19:498.

[64] Stachowicz A, Siudut J, Suski M, Olszanecki R, Korbut R, Undas A, Wiśniewski JR. Optimization of quantitative proteomic analysis of clots generated from plasma of patients with venous thromboembolism. *Clin Proteomics*. 2017;14:38.

[65] Bryk AH, Natorska J, Ząbczyk M, Zettl K, Wiśniewski JR, Undas A. Plasma fibrin clot proteomics in patients with acute pulmonary embolism: association with clot properties. *J Proteomics*. 2020;229:103946. https://doi.org/10.1016/j.jprot.2020.103946

[66] Mukherjee AK, Mackessy SP, Dutta S. Characterization of a Kunitz-type protease inhibitor peptide (Rusvikunin) purified from *Daboia russelii russelii* venom. *Int J Biol Macromol*. 2014;67:154–62.

[67] Waheed H, Moin SF F, Choudhary MI. Snake venom: from deadly toxins to life-saving therapeutics. *Curr Med Chem*. 2017;24:1874–91.

[68] Mohamed Abd El–Aziz T, Garcia Soares A, Stockand JD. Snake venoms in drug discovery: Valuable therapeutic tools for life saving. *Toxins (Basel)*. 2019;11:564.

[69] Goa KL, Noble S. Eptifibatide: a review of its use in patients with acute coronary syndromes and/or undergoing percutaneous coronary intervention. *Drugs*. 1999;57:439–62.

[70] Lange U, Olschewski A, Nowak G, Bucha E. [Ecarin chromogenic assay: an innovative test for quantitative determination of direct thrombin inhibitors in plasma]. *Hamostaseologie*. 2005.

[71] Lövgren A. Recombinant snake venom prothrombin activators. *Bioengineered*. 2013;4:153–7.

SUPPLEMENTARY MATERIAL

The online version contains supplementary material available at https://doi.org/10.1016/j.jtha.2025.03.012.